



HAL
open science

Quasi-LPV Modeling of Guided Projectile Pitch Dynamics through State Transformation Technique

Gian Marco Vinco, Spilios Theodoulis, Olivier Sename, Guillaume Strub

► **To cite this version:**

Gian Marco Vinco, Spilios Theodoulis, Olivier Sename, Guillaume Strub. Quasi-LPV Modeling of Guided Projectile Pitch Dynamics through State Transformation Technique. Joint 8th IFAC Symposium on System Structure and Control, 17th IFAC Workshop on Time Delay Systems, 5th IFAC Workshop on Linear Parameter Varying Systems, Sep 2022, Montreal, Canada. 10.1016/j.ifacol.2022.11.288 . hal-03690075

HAL Id: hal-03690075

<https://hal.univ-grenoble-alpes.fr/hal-03690075>

Submitted on 7 Jun 2022

HAL is a multi-disciplinary open access archive for the deposit and dissemination of scientific research documents, whether they are published or not. The documents may come from teaching and research institutions in France or abroad, or from public or private research centers.

L'archive ouverte pluridisciplinaire **HAL**, est destinée au dépôt et à la diffusion de documents scientifiques de niveau recherche, publiés ou non, émanant des établissements d'enseignement et de recherche français ou étrangers, des laboratoires publics ou privés.

Quasi-LPV Modeling of Guided Projectile Pitch Dynamics through State Transformation Technique

G.M. Vinco ^{*,**} S. Theodoulis ^{*} O. Sename ^{**} G. Strub ^{*}

^{*} French-German Research Institute of Saint-Louis, 68300,
Saint-Louis, France (e-mail: spilios.theodoulis@isl.eu,
guillaume.strub@isl.eu).

^{**} University Grenoble Alpes, CNRS, Grenoble INP, GIPSA-Lab,
38000, Grenoble, France (e-mail: gian-marco.vinco@grenoble-inp.fr,
olivier.sename@grenoble-inp.fr).

Abstract: In this paper, we develop a reliable *Linear Parameter-Varying* (LPV) model of the pitch channel dynamics of a fin-stabilized projectile. Among the available LPV design approaches, the *State Transformation* is analyzed, being particularly suitable for a class of systems defined as output nonlinear, and compatible with the projectile dynamics formulation. The *State Transformation* provides a quasi-LPV representation, which corresponds to an exact transformation of the original nonlinear model, preserving relevant couplings that are usually lost through the classical approximation methods. Some important considerations regarding the limitations of this approach are also discussed and verified in the missile dynamics. The accuracy of the obtained quasi-LPV model is assessed by means of open-loop simulations, comparing the performance to the original nonlinear model at selected flight conditions.

Keywords: Linear parameter-varying systems, Flight dynamics modeling, Model validation.

1. INTRODUCTION

In the field of aerospace applications, the *Linear Parameter-Varying* (LPV) framework has already provided successful results in terms of both system modeling and control design. However, it implies the nontrivial transformation process of the original nonlinear system into the corresponding LPV formulation, which requires an exhaustive investigation. A standard approach, especially for industrial settings, is based on the Jacobian linearization (Theodoulis et al. (2010), Prempain et al. (2001)). The LPV model is obtained as a collection of linearized LTI plants, where the investigated parameters are "frozen" around specific design values. Despite its feasibility, the main drawbacks of this method rely on the inability to fully capture the system dynamics away from the design points, potentially neglecting important nonlinearities and coupling terms that can affect the system behavior.

Several alternative approaches for LPV system derivation have been proposed in the last years with successful applications, such as function substitution (Pfifer (2012), and Marcos and Balas (2004)), velocity-based techniques (Leith and Leithead (1998)), and *State Transformation* (Shamma and Cloutier (1993), and Carter and Shamma (1996)). In this paper, the latter method is investigated to develop a reliable quasi-LPV model for a projectile dynamics pitch channel autopilot. The structural configuration of the projectile, and the Bank-To-Turn flight strategy intended to be implemented, may generate relevant nonlinear couplings in the projectile dynamics. The *State Transformation* method provides an exact transformation

between the original nonlinear system and the obtained quasi-LPV model, thus no approximations are involved in the design, increasing its capability to represent the original dynamics. A simplified version of the original nonlinear model is first developed. This allows to respect the requirements imposed by the *State Transformation* technique without penalizing the nonlinear coupling terms present in the dynamics. The quasi-LPV formulation derived from the simplified nonlinear model is strongly dependent on the feasible trim map and presents an internal feedback loop that updates in real-time the trimmed input at the current flight conditions. In order to avoid any stability and robustness issues, a second quasi-LPV model is generated by augmenting the system with an integrator at the input. The performance of the two quasi-LPV models is analyzed and compared with both the original nonlinear dynamics and the simplified one to assess the impact of the assumptions on the model reliability.

The investigated nonlinear model dynamics is discussed in Section 2, together with some relevant insight related to the projectile aerodynamic coefficients. Section 3 addresses more in details the structure of the output nonlinear (or output dependent) class of systems, as well as the *State Transformation* approach employed for the derivation of the quasi-LPV model. Important considerations are also discussed, with the intention of reformulating the nonlinear model in a suitable form that respects the *State Transformation* assumptions. Finally, in Section 4, open-loop simulations are performed, aiming to compare the time response of the nonlinear and quasi-LPV models and to assess the accuracy of the latter.

2. PROJECTILE NONLINEAR MODEL

The investigated concept consists of a 155 mm fin-stabilized guided projectile, equipped with a set of four symmetrical rear fins, and two horizontal front canards, in a non-coplanar configuration, as shown in Fig. 1.

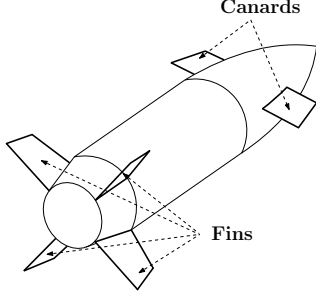


Fig. 1. Projectile concept: details on the control surfaces.

The complete nonlinear reference model has been derived in Vinco et al. (2022). The original equations of motion describing the projectile translational dynamics in the body coordinates (B) have been converted to the more convenient stability coordinates, in terms of the angle-of-attack, the sideslip-angle, and the true airspeed (zero relative wind), respectively α , β , and V , as in Zipfel (2014).

2.1 Pitch Dynamics

The proposed study focuses on the pitch channel of the projectile dynamics, intended to be analyzed in view of the future autopilot design. The projectile behavior is modeled through the dynamics of α , and the pitch rate, q :

$$\begin{aligned} \dot{\alpha} &= -\frac{X \sin \alpha}{mV \cos \beta} + \frac{Z \cos \alpha}{mV \cos \beta} \\ &+ \frac{g}{V \cos \beta} (\sin \alpha \sin \theta + \cos \alpha \cos \theta \cos \phi) \\ &+ q - p \tan \beta \cos \alpha - r \tan \beta \sin \alpha, \\ \dot{q} &= \frac{1}{I_{yy}} [M - pr (I_{xx} - I_{zz})], \end{aligned} \quad (1)$$

where m stands for the mass of the projectile, g is the acceleration of gravity, I_{xx} , I_{yy} , and I_{zz} refer to the moments of inertia about the x, y, and z axes, respectively. Additionally, p and r , correspond to the roll and yaw rates, respectively, while ϕ and θ indicate the roll and pitch angles. In particular, the air mass is assumed at rest, so no relative wind contributions are modeled and, due to the projectile planar symmetry with respect to the $x-z$ and $x-y$ planes, the products of Inertia I_{xy} , I_{yz} , and I_{xz} result to be negligible.

2.2 Aerodynamic Model

Concerning the projectile aerodynamics, the *Simple Linear* aerodynamic model discussed in Vinco et al. (2022) is here employed, in reason of the observed high fidelity level and the lower mathematical complexity. Furthermore, the influence of β on the pitch dynamics is expected to be negligible. The longitudinal and vertical forces, X and Z , and the pitching moment, M , are functions of the dynamic

pressure $\bar{q} = \frac{1}{2}\rho(h)V^2$, the reference surface S and caliber d , the air density ρ , and the altitude h , as follows:

$$\begin{aligned} X &= \bar{q}S \left(C_{X_S} + C_{X_{\delta_{\text{eff}}}} \right), \\ Z &= \bar{q}S \left[C_{Z_S} + \left(\frac{d}{V} \right) C_{Z_D} q + C_{Z_{\delta_q}} \right], \\ M &= \bar{q}Sd \left[C_{m_S} + \left(\frac{d}{V} \right) C_{m_D} q + C_{m_{\delta_q}} \right]. \end{aligned} \quad (2)$$

The projectile static coefficients, $C_{X_S}(\mathcal{M}, \alpha)$, $C_{Z_S}(\mathcal{M}, \alpha)$, and $C_{m_S}(\mathcal{M}, \alpha)$ were derived in the *Simple Linear* model as a function of the Mach number, \mathcal{M} , and the angle α . Similarly, the virtual control coefficients $C_{X_{\delta_{\text{eff}}}}(\mathcal{M}, \delta_{\text{eff}})$, $C_{Z_{\delta_q}}(\mathcal{M}, \delta_q)$, $C_{m_{\delta_q}}(\mathcal{M}, \delta_q)$ are expressed with respect to the virtual pitch δ_q , and virtual roll δ_p control deflections, their nonlinear combination $\delta_{\text{eff}} = \sqrt{\delta_p^2 + \delta_q^2}$, and the Mach number.

$$\begin{aligned} C_{X_{\delta_{\text{eff}}}} &= C_{X_{\delta_0}}(\mathcal{M}) + C_{X_{\delta_2}}(\mathcal{M}) \sin^2 \delta_{\text{eff}}, \\ C_{Z_{\delta_q}} &= C_{Z_{\delta_1}}(\mathcal{M}) \sin \delta_q + C_{Z_{\delta_3}}(\mathcal{M}) \sin^3 \delta_q, \\ C_{m_{\delta_q}} &= C_{m_{\delta_1}}(\mathcal{M}) \sin \delta_q + C_{m_{\delta_3}}(\mathcal{M}) \sin^3 \delta_q. \end{aligned} \quad (3)$$

In particular, the virtual deflections δ_p and δ_q , are generated by the mutual interactions between the individual right and left canard deflections, δ_r and δ_l , respectively. As shown in Figs. 2a - 2b, the virtual roll is defined by the differential deflection $\delta_p = \frac{\delta_l - \delta_r}{2}$, while the virtual pitch by the concurrent deflection $\delta_q = \frac{\delta_l + \delta_r}{2}$, respectively.

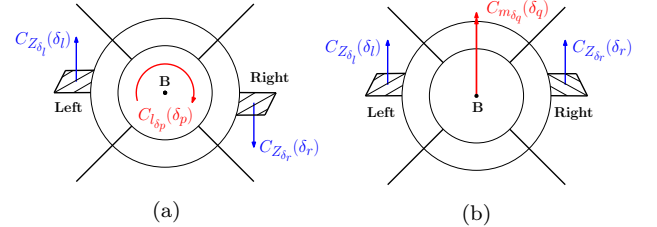


Fig. 2. Individual and virtual control deflections: (a) virtual roll, (b) virtual pitch.

Coherently, the virtual control coefficients were modeled as an approximation of the global coefficients:

$$\begin{aligned} C_{Z_{\delta}} &= C_{Z_{\delta_r}}(\mathcal{M}, \delta_r) + C_{Z_{\delta_l}}(\mathcal{M}, \delta_l), \\ C_{m_{\delta_q}} &= C_{m_{\delta_r}}(\mathcal{M}, \delta_r) + C_{m_{\delta_l}}(\mathcal{M}, \delta_l), \end{aligned} \quad (4)$$

generated by the linear superposition of the individual canard contributions. The derivation is extensively discussed in Vinco et al. (2022). An interpolation analysis was conducted to define the deflection range in which the canards response results to be linear, motivating the superposition of the individual deflections in a combined contribution. The results exhibited a reliable level of accuracy for the deflection range $\delta_r, \delta_l \in [-25^\circ, 25^\circ]$.

Finally, the aerodynamic damping coefficients $C_{Z_D}(\mathcal{M}, \alpha)$ and $C_{m_D}(\mathcal{M}, \alpha)$ are also addressed in the model, aiming to provide with an exhaustive characterization of the projectile behavior.

3. QUASI-LPV MODELING

Linear Parameter-Varying refers to a class of systems whose state space representation is defined as a continuous function of a time-varying vector of scheduling parameters ρ^1 , assumed to be measurable in real-time. For a detailed definition, the reader can refer to Sename et al. (2013) and Mohammadpour and Scherer (2012). When the state of the system, x , is decomposed into a scheduling subset, $z(t)$, and a nonscheduling subset $w(t)$, the system is specifically indicated as quasi-LPV. Coherently, the scheduling parameters are divided into an exogenous subset, $\Omega(t)$, and an endogenous subset, $z(t)$.

$$x(t) = [z(t) \quad w(t)]^T, \quad \rho(t) = [z(t) \quad \Omega(t)]^T.$$

3.1 State Transformation

The approach was first introduced in Shamma and Cloutier (1993) and later further elaborated in Leith and Leithead (2000). It consists of a state transformation aimed to remove all the nonlinearities present in the model, that do not depend on the scheduling variables. As extensively discussed in Leith and Leithead (2000), the *State Transformation* is suitable for a restricted class of systems, defined as *Output Nonlinear* or *Output Dependent*, and expressed in the generic form:

$$\begin{aligned} \begin{bmatrix} \dot{z} \\ \dot{w} \end{bmatrix} &= \begin{bmatrix} f_1(\rho) \\ f_2(\rho) \end{bmatrix} + \begin{bmatrix} A_{11}(\rho) & A_{12}(\rho) \\ A_{21}(\rho) & A_{22}(\rho) \end{bmatrix} \begin{bmatrix} z \\ w \end{bmatrix} + \begin{bmatrix} B_1(\rho) \\ B_2(\rho) \end{bmatrix} u, \\ y &= z, \end{aligned} \quad (5)$$

where $u(t) \in \mathbb{R}^{n_u}$ represents the control input, and the model nonlinearities $f_1(\rho)$ and $f_2(\rho)$, appear only as a function of the measured output $z(t) \in \mathbb{R}^{n_z}$, and of a selected set of exogenous parameters $\Omega(t)$.

The transformation is achieved by means of trimming functions of the nonscheduling states $w(t)$, and of the control input, assuming that $n_z = n_u$. By considering a feasible trim region of the flight envelope, where the trimming functions $w_{\text{eq}}(\rho)$ and $u_{\text{eq}}(\rho)$, respectively, are continuously differentiable for every z and ρ , such that:

$$\begin{aligned} \begin{bmatrix} 0 \\ 0 \end{bmatrix} &= \begin{bmatrix} f_1(\rho) \\ f_2(\rho) \end{bmatrix} + \begin{bmatrix} A_{11}(\rho) & A_{12}(\rho) \\ A_{21}(\rho) & A_{22}(\rho) \end{bmatrix} \begin{bmatrix} z \\ w_{\text{eq}}(\rho) \end{bmatrix} \\ &+ \begin{bmatrix} B_1(\rho) \\ B_2(\rho) \end{bmatrix} u_{\text{eq}}(\rho), \end{aligned} \quad (6)$$

and by defining the new set of transformed entries:

$$\begin{aligned} \xi(t) &:= w(t) - w_{\text{eq}}(\rho(t)), \\ \nu(t) &:= u(t) - u_{\text{eq}}(\rho(t)), \\ \tilde{A}_{22}(\rho) &:= A_{22}(\rho) - \frac{\partial w_{\text{eq}}}{\partial z} A_{12}(\rho), \\ \tilde{B}_2(\rho) &:= B_2(\rho) - \frac{\partial w_{\text{eq}}}{\partial z} B_1(\rho), \\ E(\rho) &:= -\frac{\partial w_{\text{eq}}}{\partial \Omega}, \end{aligned} \quad (7)$$

the original nonlinear system in (5) can be reformulated as a quasi-LPV model, in the form:

$$\begin{bmatrix} \dot{z} \\ \dot{\xi} \end{bmatrix} = \begin{bmatrix} 0 & A_{12}(\rho) \\ 0 & \tilde{A}_{22}(\rho) \end{bmatrix} \begin{bmatrix} z \\ \xi \end{bmatrix} + \begin{bmatrix} B_1(\rho) \\ \tilde{B}_2(\rho) \end{bmatrix} \nu + \begin{bmatrix} 0 \\ E(\rho) \end{bmatrix} \dot{\Omega}. \quad (8)$$

In particular, the additional input term $\dot{\Omega}$ describes the impact of the dynamics of the exogenous variables on the system, through the trimming functions. For the current analysis, this term can be assumed as a disturbance to be rejected and thus neglected in the model, as discussed in Balas (2002). However, it represents an interesting aspect to be further investigated for future works.

The dependence of this formulation on the feasible trim map can be inferred from (7). Indeed, the definition of the deviated input ν depends on the selected equilibrium condition u_{eq} . From a stability and robustness perspective, this internal feedback loop may affect the performance of the system and the following control design. Thus, a straightforward solution would be to require that the trimmed input $u_{\text{eq}}(\rho) = 0$, imposing a strong limitation to the region of the trim map that respects this condition.

An interesting design alternative consists of adding an integrator at the plant input. By defining, $u = \int \sigma$, we can reformulate the system (8), as:

$$\begin{bmatrix} \dot{z} \\ \dot{\xi} \\ \dot{\nu} \end{bmatrix} = \begin{bmatrix} 0 & A_{12}(\rho) & B_1(\rho) \\ 0 & \tilde{A}_{22}(\rho) & \tilde{B}_2(\rho) \\ 0 & \tilde{A}_{32}(\rho) & \tilde{B}_3(\rho) \end{bmatrix} \begin{bmatrix} z \\ \xi \\ \nu \end{bmatrix} + \begin{bmatrix} 0 \\ 0 \\ I \end{bmatrix} \sigma, \quad (9)$$

with:

$$\tilde{A}_{32}(\rho) := -\frac{\partial u_{\text{eq}}}{\partial z} A_{12}(\rho); \quad \tilde{B}_3(\rho) := -\frac{\partial u_{\text{eq}}}{\partial z} B_1(\rho). \quad (10)$$

In this way, the new input is uniformly zero at every equilibrium point and the feedback loop does not affect the system anymore. Furthermore, this solution is motivated by the assumption that the controller intended to be designed contains pure integral action for steady state tracking error elimination. Thus, the controller integral action can be formally included in the system description.

The main advantage of the *State Transformation* approach relies on the exact transformation between the original nonlinear system and the obtained quasi-LPV model, which avoids any form of approximation, as opposed to the classical Jacobian linearization. Additionally, due to the integration of the control input, the reliability of the quasi-LPV model does not depend on the specific operating point, and the term $\dot{w}_{\text{eq}} = \frac{\partial w_{\text{eq}}}{\partial z} \dot{z}$, included in (7), allows to account for any off-equilibrium conditions.

3.2 Pitch Channel quasi-LPV Model

As previously mentioned, the *State Transformation* approach results to be very suitable for aerospace application. It is easy to observe how the pitch channel dynamics, presented in (1), is already formulated as the *Output Nonlinear* system in (5). In particular, the state variables $[z, w]^T = [\alpha, q]^T$ represent the measured and the

¹ The scheduling parameters set ρ used in Sections 3 - 4 is different from the air density, $\rho(h)$, defined in Section 2.

unmeasured output, respectively, while the set of varying parameters intended to be investigated corresponds to $[z, \Omega]^T = [\alpha, (V, h)]^T$, being α and $[V, h]$ the endogenous and the exogenous variables, respectively.

The reader can notice in the complete projectile nonlinear model in Vinco et al. (2022), that the true airspeed V was defined through its components along the main body coordinates, $[u_B, v_B, w_B]^T$, included in the model state. Thus, V itself could be considered as a state for the pitch dynamics, describing the long period longitudinal dynamics (phugoid) of the projectile. However, because of the lack of any relevant control authority on the projectile longitudinal velocity, u_B , V is addressed in this paper as an exogenous scheduling variable. As implied by the *Output Nonlinear* formulation, all the nonlinearities involved in the model are expressed as a function of the measured output. The only exceptions rely on the control coefficient definitions in (3). Indeed, $(C_{X_{\delta_{\text{eff}}}}, C_{Z_{\delta_q}}, C_{m_{\delta_q}})$ are modeled as nonlinear functions of the virtual control inputs δ_q and δ_p . Consequently, the system is not affine with respect to the control inputs.

In order to adjust the projectile dynamics into a suitable form, a correction of the control terms is required. To avoid any approximation through a standard Taylor expansion, the aerodynamics data analyzed in Vinco et al. (2022) have been investigated with a lower order regression model. In particular, in Figs. 3a - 3b, the vertical force, and pitching moment canards coefficients (symmetrical for the individual right and left canard deflections, δ_r and δ_l) exhibit a linear response for a bounded range of deflections. (The reader should notice that all the presented data have been normalized in reason of confidentiality.)

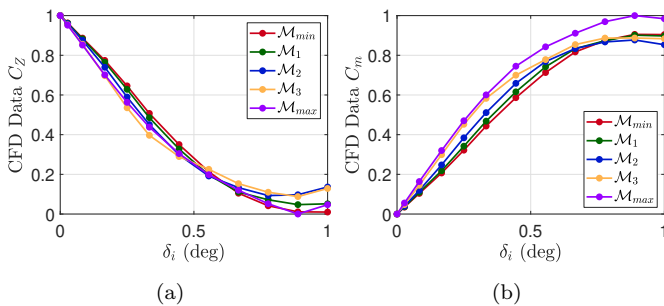


Fig. 3. Canards response for deflection δ_i , $i = r, l$: (a) vertical force coefficient, (b) pitching moment coefficient. (All the data have been normalized in reason of confidentiality.)

By restricting the analysis to the deflections range (normalized) $\delta_r, \delta_l \in [-0.7^\circ, 0.7^\circ]$, and by employing the first order regression models $C_{Z_{\delta_r}} = C_{Z_{\delta_1}} \delta_r$, and $C_{m_{\delta_r}} = C_{m_{\delta_1}} \delta_r$, the obtained accuracy results higher than 95% in terms of *Coefficient of Determination*, for both the coefficients. The same results are observed for the left canard deflection. As discussed in Vinco et al. (2022), a second analysis is then performed in order to model the resulting global coefficients as in (4), into the corresponding virtual formulations $(C_{Z_{\delta_q}}, C_{m_{\delta_q}})$.

The interpolation error is expressed in terms of the difference between the global coefficients and the virtual ones, normalized by the value of the original aerodynamic

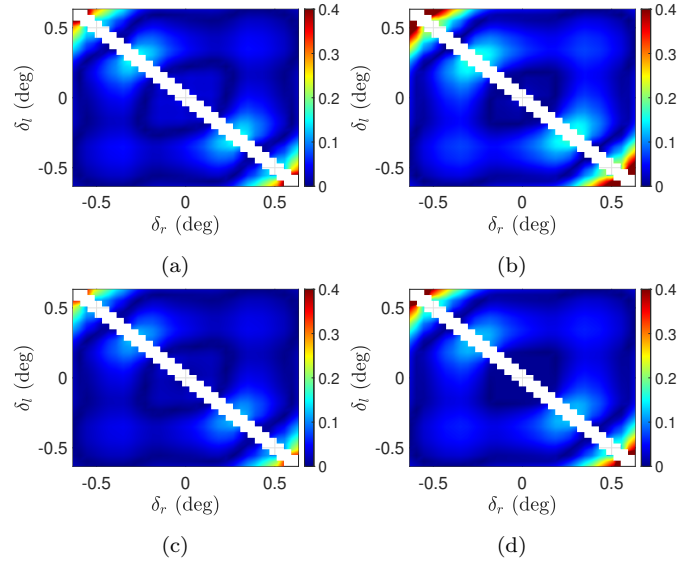


Fig. 4. Interpolation error: (a) - (b) vertical force coefficient at different Mach values; (c) - (d) pitching moment coefficient at different Mach values. (All the data have been normalized in reason of confidentiality.)

data. As shown in Fig. 4, both the vertical force and the pitching moment exhibit an average error lower than 10% in the investigated deflection range. Thus, the control coefficients can be reformulated in a way to be affine with respect to the pitch dynamics. The longitudinal control force, $C_{X_{\delta_{\text{eff}}}}$, nonlinear function of δ_p and δ_q , is neglected for the purposes of this analysis. The choice is motivated by the intent to operate in a gliding flight condition, a subsonic regime, where the drag generated by the canard deflections does not provide a relevant impact on the projectile aerodynamics.

4. MODEL VALIDATION

In order to assess the reliability of the obtained quasi-LPV model, a campaign of open-loop simulations has been performed. The scheduling parameters investigated during the analysis are $\rho = [\alpha, V]$, while the altitude h is assumed as constant. In particular, for each combination of the parameters, the corresponding trimming functions $w_{\text{eq}}(\rho) = q_{\text{eq}}(\rho)$ and $u_{\text{eq}}(\rho) = \delta_{q,\text{eq}}(\rho)$ are evaluated to define the initial equilibrium condition of the simulation. The analysis shown in Figs. 5a - 5b provide a map of the equilibrium points variation as a function of the scheduling parameter.

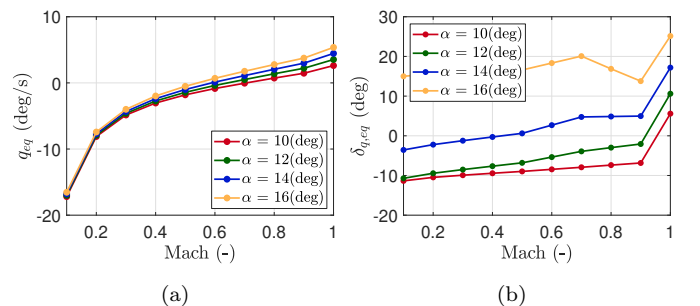


Fig. 5. Trimming functions analysis: (a) pitch rate equilibrium values; (b) control deflection equilibrium values.

The ranges of variation of the angle of attack correspond to $\alpha \in [10^\circ, 16^\circ]$, coherently with the assumption of a smooth gliding flight strategy. The velocity range is expressed in terms of the equivalent Mach values, since the intent is to investigate the performance in the subsonic regime, $\mathcal{M} \in [0.1, 1]$. The conversion is based on the relation $V = \mathcal{M}a$, where the speed of sound, a , is constant due to the assumption of constant altitude. In reason of the projectile stability limitations discussed in Vinco et al. (2022), and the lower equilibrium deflection commands observed in Fig. 5b, the equilibrium conditions considered for the following performance comparison are shown in Tab. 1. Indeed, the low equilibrium deflection, $\delta_{q,eq}$, allows the employment of a larger input command as a form of perturbation to the system, without exceeding the validity range of the aerodynamic model.

Table 1. Trim point and equilibrium conditions.

$\alpha(deg)$	$V(m/s)$	$h(m)$	$q_{eq}(deg/s)$	$\delta_{q,eq}(deg)$
14	158.026	6029	-1	0.6

In the following sections, both the quasi-LPV model formulated as in (8), with the internal feedback loop affecting the control input, and the Augmented quasi-LPV model as in (9) assuming integral action on the input, are investigated. In particular, their open-loop responses are compared to the ones of the original complete nonlinear model (NL), including the aerodynamics in (3), and the simplified one (NL_{sim}), presenting the linear aerodynamic model discussed in Section 3.

4.1 Quasi-LPV Model

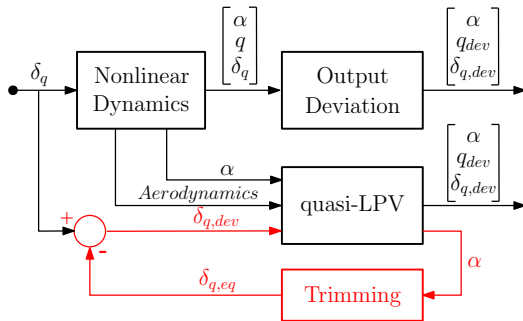


Fig. 6. Quasi-LPV model design scheme.

The simulation is performed assuming the initial equilibrium conditions in Tab. 1, and a set of input commands corresponding to a first deflection $\delta_{q_1} = 20^\circ$ at $t_1 = 5$ s, and second deflection of $\delta_{q_2} = -15^\circ$ at $t_2 = 30$ s. The results in Fig. 7a - 7c show the open-loop time responses related to the transformed states $\alpha(t)$ and $q_{dev}(t) = q(t) - q_{eq}(t)$, and to the transformed input $\delta_{q,dev}(t) = \delta_q(t) - \delta_{q,eq}(t)$, respectively. In particular, the $q_{dev}(t)$ and the $\delta_{q,dev}(t)$ of the nonlinear models, are obtained in post processing by applying the transformation to the original state $q(t)$, and input $\delta_q(t)$, of the system, as shown in Fig. 6.

The curves describing the quasi-LPV (q-LPV) and the simplified nonlinear model (NL_{sim}) are perfectly overlapped since the former has been obtained through an exact transformation of the latter. On the other side, a small mismatch in the convergence values is observed

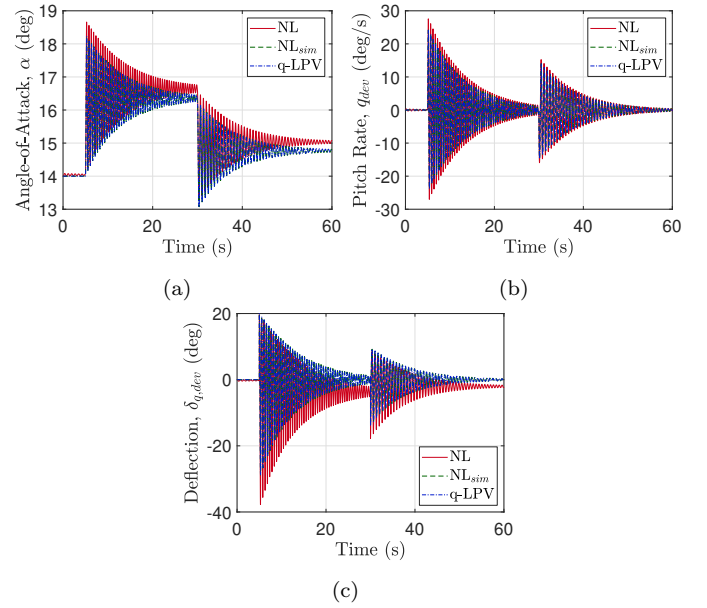


Fig. 7. Simulation time responses: (a) angle-of-attack; (b) deviated pitch rate; (c) deviated input deflections.

with respect to the full nonlinear model (NL), because of the different aerodynamics. For the same reason, the NL model shows some initial oscillations around the equilibrium conditions, which have been evaluated on the base of the NL_{sim} model. The results in Tab. 2 present the Root Mean Square Error (RMSE) evaluated between the three models for each of the state variables, and normalized by the maximum variation range of each state variable related to the NL model. In particular, the RMSE values obtained between the NL_{sim} and the q-LPV models are very small, while the others are almost the same, coherently to what previously observed in the simulation results.

Table 2. RMSE results: quasi-LPV model.

	NL - q-LPV	NL _{sim} - q-LPV	NL - NL _{sim}
α	0.1302	0.0018	0.1310
q_{dev}	0.1332	0.0020	0.1342
$\delta_{q,dev}$	0.1352	0.0019	0.1361

The large oscillations characterizing all the three responses can be associated with the stability of the projectile dynamics since, at the flight conditions in Tab. 1, the system is near the limit of static stability.

4.2 Augmented quasi-LPV Model

The same simulation is performed on the Augmented quasi-LPV model. The main difference consists of the input commands (δ_{q_1} , δ_{q_2}) that are injected into the

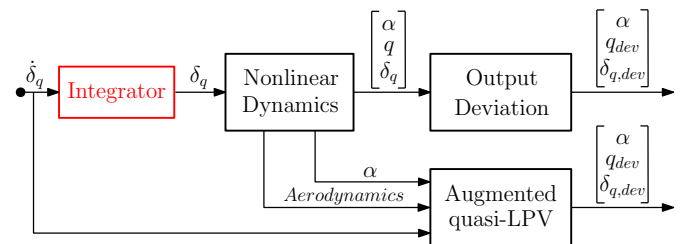


Fig. 8. Augmented quasi-LPV model design scheme.

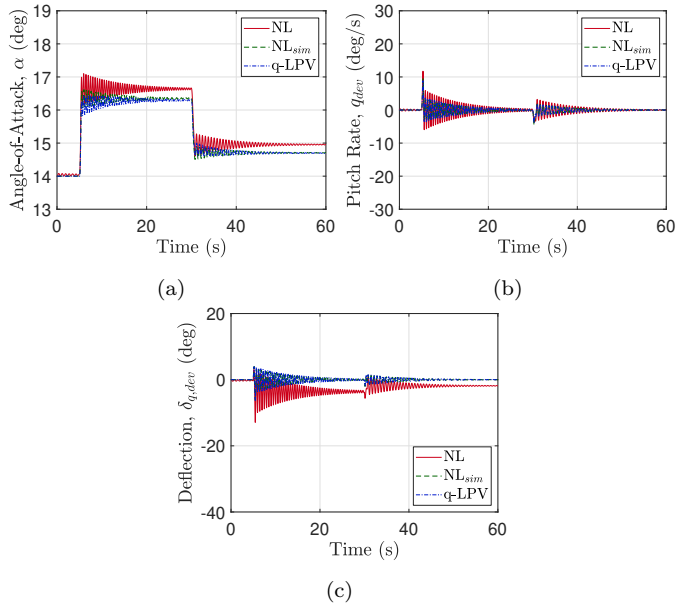


Fig. 9. Simulation time responses: (a) angle-of-attack; (b) deviated pitch rate; (c) deviated input deflections.

systems since the input now are integrated for both the quasi-LPV and the nonlinear models². In this context, two pulses simulating the canards deflection rates ($\dot{\delta}_{q_1}$, $\dot{\delta}_{q_2}$) are employed as perturbations. The deflection rates are selected such that, once integrated, they provide the same control deflection (δ_{q_1} , δ_{q_2}), previously defined. The curves in Figs. 9a - 9c, related to the Augmented q-LPV and the NL_{sim} models, present a mild difference due to the way the integrator is implemented. Indeed, in the former system, the deflection is accounted for as a state, thus the integrator is part of the internal dynamics. Differently, in the two nonlinear systems the integral action is applied to the input before being injected into the system.

Table 3. RMSE results: Augmented quasi-LPV model.

	NL - qLPV	NL_{sim} - qLPV	NL - NL_{sim}
α	0.0968	0.0373	0.0913
q_{dev}	0.0341	0.0585	0.0805
$\delta_{q,dev}$	0.1705	0.0655	0.1886

The main advantage of the Augmented formulation consists in the removal of the internal loop updating the trimming values. As previously discussed, it can be critical in terms of performance since any forms of unmodeled dynamics or approximation are injected as input disturbances. Additionally, the RMSE values in Tab. 3 show a better accuracy between the Augmented q-LPV model and the NL one with respect to the results in Tab. 2, confirming the improvement of the augmented formulation. The differences between the NL and the NL_{sim} models, generated by the aerodynamics approximations, appear to be reduced by the integration process. The only exception relies on deviated deflection, $\delta_{q,dev}$, where the integration tends to increase the bias in the convergence values. Finally, it is interesting to observe how the convergence values for the three states are almost the same as the ones in Figs. 7a - 7c, but the oscillation amplitudes are way narrower.

² An integrator is added at the nonlinear system input to be consistent with the q-LPV formulation during the comparison.

5. CONCLUSION

In this paper, the pitch dynamics of a guided projectile in investigated. The nonlinear model is converted through the *State Transformation* approach into two quasi-LPV models. The first model, (quasi-LPV), presents a strong dependence on the trim map due to an internal loop updating the system input. In the second one, (Augmented quasi-LPV), this issue is addressed by augmenting the system with an integrator at the input. Open-loop simulation results and RMSE analysis show higher accuracy in the case of the augmented system. This model will be employed for the development of a LPV-based pitch autopilot.

REFERENCES

- Balas, G.J. (2002). Linear, parameter-varying control and its application to aerospace systems. In *Proceedings of the ICAS congress*. Toronto, Canada.
- Carter, L.H. and Shamma, J.S. (1996). Gain-scheduled bank-to-turn autopilot design using linear parameter varying transformations. *Journal of guidance, control, and dynamics*, 19(5), 1056–1063.
- Leith, D.J. and Leithead, W. (1998). Gain-scheduled and nonlinear systems: dynamic analysis by velocity-based linearization families. *International Journal of Control*, 70(2), 289–317.
- Leith, D.J. and Leithead, W.E. (2000). Survey of gain-scheduling analysis and design. *International journal of control*, 73(11), 1001–1025.
- Marcos, A. and Balas, G.J. (2004). Development of linear-parameter-varying models for aircraft. *Journal of Guidance, Control, and Dynamics*, 27(2), 218–228.
- Mohammadpour, J. and Scherer, C.W. (2012). *Control of linear parameter varying systems with applications*. Springer Science & Business Media.
- Pfifer, H. (2012). Quasi-LPV model of a NDI-controlled missile based on function substitution. In *Proceedings of the AIAA Guidance, Navigation, and Control Conference*, 4970. Minneapolis, MN, USA.
- Prempain, E., Postlethwaite, I., and Vorley, D. (2001). A gain scheduled autopilot design for a bank-to-turn missile. In *Proceedings of the 2001 European Control Conference (ECC)*, 2052–2057. IEEE, Porto, Portugal.
- Sename, O., Gaspar, P., and Bokor, J. (2013). *Robust control and linear parameter varying approaches: application to vehicle dynamics*, volume 437. Springer.
- Shamma, J.S. and Cloutier, J.R. (1993). Gain-scheduled missile autopilot design using linear parameter varying transformations. *Journal of guidance, Control, and dynamics*, 16(2), 256–263.
- Theodoulis, S., Morel, Y., Wernert, P., and Tzes, A. (2010). LPV modeling of guided projectiles for terminal guidance. In *Proceedings of the 18th Mediterranean Conference on Control and Automation, MED'10*, 1455–1460. IEEE, Marrakech, Morocco.
- Vinco, G.M., Theodoulis, S., and Sename, O. (2022). Flight dynamics modeling and simulator design for a new class of long-range guided projectiles. In *CEAS EuroGNC Conference*. Berlin, Germany. URL <https://hal.univ-grenoble-alpes.fr/hal-03654390>.
- Zipfel, P.H. (2014). *Modeling and Simulation of Aerospace Vehicle Dynamics*. American Institute of Aeronautics and Astronautics, Inc., 3rd edition.